Volume 218, number 1, 178–184 FEB 04821 June 1987

The structure of mouse L1210 dihydrofolate reductase-drug complexes and the construction of a model of human enzyme

D.K. Stammers, J.N. Champness, C.R. Beddell, J.G. Dann, E. Eliopoulos[+], A.J. Geddes[+], D. Ogg[+] and A.C.T. North[+]

Wellcome Research Laboratories, Beckenham, BR3 3BS and
[+] *Astbury Department of Biophysics, University of Leeds, Leeds LS2 9JT, England*

Received 9 April 1987

The structure of mouse L1210 dihydrofolate reductase (DHFR) complexed with NADPH and trimethoprim has been refined at 2.0 Å resolution. The analogous complex with NADPH and methotrexate has been refined at 2.5 Å resolution. These structures reveal for the first time details of drug interactions with a mammalian DHFR, which are compared with those observed from previous X-ray investigations of DHFR/inhibitor complexes. The refined L1210 structure has been used as the basis for the construction of a model of the human enzyme. There are only twenty-one sequence differences between mouse L1210 and human DHFRs, and all but two of these are located close to the molecular surface: a strong indication that the active sites are essentially identical in these two mammalian enzymes.

Crystal structure; Drug-enzyme interaction; Dihydrofolate reductase

1. INTRODUCTION

Dihydrofolate reductase (DHFR) catalyses the NADPH-dependent reduction of dihydrofolate to tetrahydrofolate thereby maintaining the pool of tetrahydrofolate-derived coenzymes that are utilised in various one-carbon transfer reactions [1]. A number of clinically important drugs act through inhibition of DHFR. Thus the antibacterial, trimethoprim (TMP) inhibits bacterial DHFR selectively, showing about 3000-fold less affinity for mammalian DHFRs [2]. Methotrexate (MTX) shows high affinity for a wide range of DHFRs from different species, including mammalian enzyme [3], and is used as an anti-cancer agent.

Correspondence address: D.K. Stammers, Wellcome Research Laboratories, Beckenham BR3 3BS, England

The three-dimensional structures of DHFRs from several sources have been extensively studied [4–11]. In order to understand better the structural basis of drug selectivity and to apply this knowledge to the design of novel inhibitors, an X-ray study of DHFR from mouse L1210 tumour cells was undertaken. This enzyme shows considerably higher sequence homology with human DHFR [12] than any other DHFR structure reported. A preliminary report of the L1210 DHFR/NADPH/TMP structure at 2.5 Å resolution has already been given [13]. The data have now been extended to 2.0 Å and the structure refined. The MTX ternary complex has been refined at 2.5 Å. These studies have provided detailed information on drug-enzyme interactions in the mammalian system. Further, a model of human DHFR has been built, based on the refined L1210 structure and the human sequence.

Published by Elsevier Science Publishers B.V. (Biomedical Division)
00145793/87/$3.50

2. MATERIALS AND METHODS

DHFR prepared from L1210 cells [13] was dialysed against TMP and NADPH (1 mM) in 50 mM Hepes (Na^+), pH 7.8; the enzyme (20 mg/ml) was then crystallised by vapour diffusion, polyethylene glycol 6000 being used as the precipitant (8–24%, w/v). The space group of the crystals was $P2_1$ with unit cell dimensions a = 43.7 Å, b = 61.6 Å, c = 41.9 Å and β = 116.3°, with a single molecule per asymmetric unit. Data were collected to 2.0 Å resolution from a single crystal by means of an automatic oscillation camera [14]. Crystals of the DHFR/NADPH/MTX complex, which diffracted to 2.5 Å resolution, were prepared by soaking pre-grown crystals in 1 mM MTX, to displace TMP.

The model derived from the earlier 2.5 Å resolution map [13], phased with two isomorphous heavy atom derivatives, was used as the starting-point for refinement by the restrained least-squares method of Hendrickson and Konnert [15]. The current model is a result of three rounds of reconstruction, by means of a VAX version of the modelling program FRODO [16], together with least-squares refinement iterated to convergence after each round of rebuilding. An Evans and Sutherland PS300 display system fitted with a Leeds University liquid crystal stereo-viewer was used for the modelling process. The DHFR/NADPH/TMP model has an R value of 0.18 for data from 10 Å to 2.0 Å resolution, and the mean uncertainty in atomic position is 0.1 Å. All 1519 non-hydrogen protein atoms are contained in the model, together with 48 NADPH atoms, 21 TMP atoms and 290 water molecules. This model was used as the starting point for refinement of the MTX ternary complex. Three rounds of building and refinement, as for TMP, incorporating data from 10 Å to 2.5 Å, resulted in a final R value of 0.19.

3. RESULTS AND DISCUSSION

3.1. *Trimethoprim binding*

The binding of TMP to mouse L1210 enzyme, depicted in fig.1, is essentially similar to that reported [7,17] for a range of substituted benzylpyrimidines, including TMP, in complex with chicken liver enzyme. Specific points to be discussed for L1210 DHFR concern the conformation of Phe-31 and the interactions of TMP with the adjacent active site residues.

The Phe-31 side-chain has torsion angles of −165° for N-Cα-Cβ-Cγ and 78° for Cα-Cβ-Cγ-Cδ. This conformation places its aromatic moiety in van der Waals contact with side-chains Phe-34 and Gln-35, and with the p-methoxy group of TMP. The ligand itself is located in the enzyme active site such that the N1 and 2-amino groups of the diaminopyrimidine form hydrogen bonds to Glu-30, the 2-amino group makes a hydrogen bond with Thr-136 via a water molecule, and the 4-amino group hydrogen bonds to the carbonyl of Ile-7. The carbonyl oxygen of Val-115 is too distant from the 4-amino group for a hydrogen bond to be made. The latter feature is similar to the case of chicken enzyme and contrasts with that of *E. coli* enzyme [7,8]. Ile-7 and Val-115 carbonyl oxygens of mouse DHFR are in fact about 0.6 Å further apart than those of the equivalent *E. coli* DHFR residues. Such a separation in mouse DHFR allows the hydroxyl group of Tyr-121 to lie quite close to the 4-amino nitrogen and to the carbonyl oxygen of Ile-7, and to hydrogen bond with the latter. The diaminopyrimidine group makes van der Waals interactions with the side-chains of Ile-7, Ala-9 and Phe-34, with the main-chain of Val-8, with the Tyr-121 hydroxyl group and with the carbonyl oxygen of the nicotinamide moiety of NADPH. TMP has torsion angles of −96° (C4-C5-C7-C1′) and 85° (C5-C7-C1′-C2′) with the valence angle at the methylene opened out to 119°, a larger value than is observed for any of the five TMP structures in the Cambridge Crystallographic Data-Base, whose average value is 115.1°. The TMP conformation is close to one of three possible solutions proposed from NMR studies of the L1210 DHFR/TMP complex [11]. As a consequence of the TMP geometry, van der Waals interactions occur between the trimethoxybenzene group and the side-chains of Leu-22, Phe-31, Phe-34, Ile-60 and Val-115.

The TMP binding described above has features akin to the interaction between the isopropenyl isostere of TMP and chicken DHFR [17]. In the interaction of TMP with chicken DHFR [7], by comparison with mouse DHFR, the C5-C7-C1′-C2′ torsion angle of TMP is about 20° greater. Furthermore, the two Tyr-31 torsion angles (about −75° and 180°) completely relocate the side-

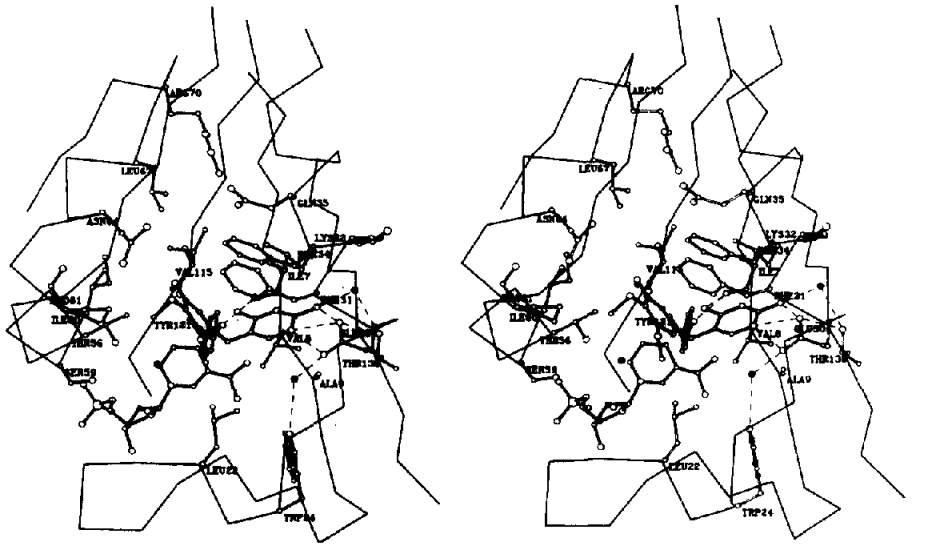

Fig.1. Stereo-view of trimethoprim complexed with mouse L1210 DHFR and NADPH. The skeletal molecular structure of the ligands and the enzyme active site are shown superimposed on an α-carbon enzyme backbone.

chain, relative to the position of the corresponding Phe-31 side-chain in the mouse DHFR, so that its hydroxyl group hydrogen bonds via a water molecule to the carbonyl oxygen of Trp-24. The energy difference for these two Tyr-31 conformations is probably small [17]. The relocation is readily accommodated given the slight change in ligand folding. The opened-out methylene valence angle of TMP in the mouse DHFR complex appears to be necessary to optimise the additional van der Waals contact of the drug with the side-chain of Phe-31.

From a comparison of interatomic distances around the active sites of both chicken and *E. coli* enzymes, Matthes et al. [17] showed that the vertebrate active site is significantly larger than the bacterial, and deduced that TMP binding in vertebrate enzyme in a conformation similar to that found in *E. coli* enzyme would not be energetically favourable. A similar comparison (table 1) between L1210 and *E. coli* enzymes of certain active site interatomic distances indicates once again a larger active site for the vertebrate enzyme than for the bacterial enzyme, though further inspection of these data by reference to table III of Matthews et al. [17] suggests that of the two vertebrate sites, the mouse active site is somewhat smaller. A significant difference in secondary structure between bacterial and vertebrate enzyme is also demonstrated by table 1. The difference distances involving residue 31 are all smaller, most by several tenths of an Ångstrom, than the corresponding differences involving the adjacent residue 30. In fact there is a distortion of the helix in this region of the vertebrate structure that is not present in *E. coli* enzyme.

3.2. *Methotrexate binding*

The binding of the pteridine moiety of MTX (see fig.2) is similar to that observed in bacterial DHFRs, despite some differences in the overall shape and size of the active site. Thus there are hydrogen-bond interactions between N1 and the carboxylate group of Glu-30, analogous to Asp-27 in *E. coli* enzyme (ec), between the 2-amino group and Glu-30, between the 2-amino group and Thr-136 via a water molecule (cf. Thr-113ec), and between the 4-amino group and the backbone carbonyl oxygens of Ile-7 and Val-115 (cf. Ile-7ec and Ile-94ec). This last interaction with mouse DHFR is not observed for TMP, as indicated earlier, which undoubtedly contributes to the relatively weak interaction of that drug with mammalian DHFR. A conserved water molecule forms a hydrogen-bond bridge from the carboxylate group of Glu-30 to the side-chain of Trp-24 (cf. Trp-22ec).

There are a number of non-polar interactions

Table 1

Table of difference distances for certain DHFR active-site atoms

	Cα-7	Cα-30	Cα-31	Cα-34	Cα-60	Cα-67	Cα-115
Cα-136	−0.13	+1.10	+0.05	−0.16	+1.15	+0.17	+0.27
Cα-115	+0.11	+1.35	+0.18	+0.16	+0.67	−0.34	
Cα-67	−0.50	+0.79	+0.50	+0.17	+0.77		
Cα-60	+0.62	+1.56	+1.02	+0.85			
Cα-34	−0.34	+0.43	−0.26				
Cα-31	−0.38	0.00					
Cα-30	+0.89						

The differences are $D(m) - D(c)$, where D is the distance (Å) between a pair of α-carbons in either mouse L1210 DHFR (m) or *E. coli* DHFR (c). The numbers denote Cα positions based on the sequence for mouse enzyme

between the pteridine ring and mouse DHFR, involving the side-chains of Ile-7, Ala-9, Leu-22, Phe-31 and Phe-34, and backbone atoms of Val-8 and Ala-9. The main differences observed from bacterial DHFRs concern the relative positions of the side-chains of Leu-28ec and Phe-31ec (Leu-27 and Phe-30 in *Lactobacillus casei* enzyme) which are approximately perpendicular to each other, whereas the corresponding side-chains in mouse DHFR (Phe-31 and Phe-34) are approximately parallel.

The *p*-aminobenzoyl group of MTX is surrounded by hydrophobic groups. On one side, the ring is in contact with the side-chains of Phe-31 and Phe-34. Apparently as a consequence of the different orientation of Phe-31 relative to the counterpart *E. coli* Lue-28ec side-chain, the benzoyl group is rotated by approx. 60° compared to its orientation in the bacterial enzyme. This in turn alters the contacts made by the opposite face of the ring. Thus the van der Waals interaction with Leu-54ec of *E. coli* enzyme is not observed for mouse enzyme. A further interaction in *E. coli* enzyme, between Arg-52ec and the benzoyl oxygen of MTX, is not observed for mouse DHFR owing to a three-residue insertion of Glu-Lys-Asn (residues 62–64) which alters the position of the analogous Arg-65. (A single insertion in *L. casei* enzyme at

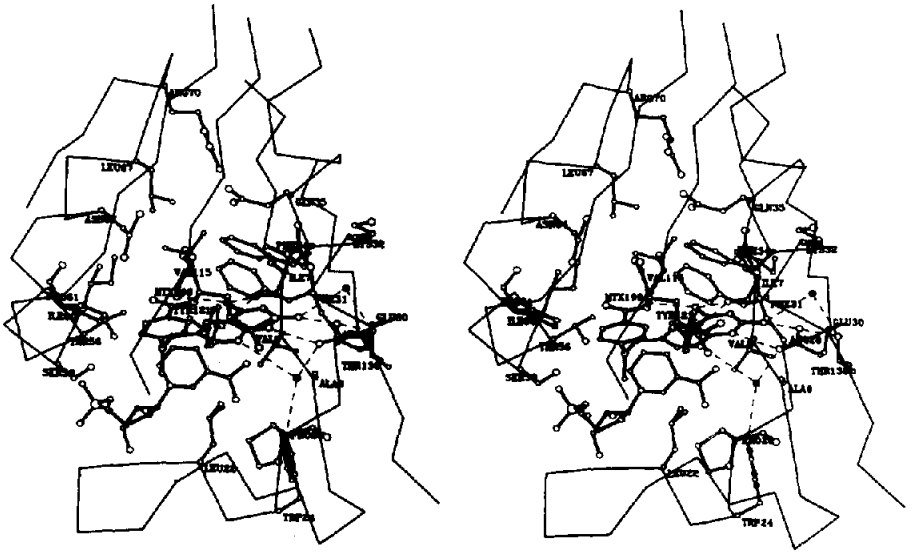

Fig.2. Methotrexate complexed with mouse L1210 DHFR and NADPH. The view is similar to that shown in fig.1.

residue 51 likewise causes an alteration to the backbone conformation so that this same interaction is lost.)

The binding of the glutamyl moiety of MTX is less clearly defined in the structure than are the pteridine or *p*-aminobenzoyl parts. The most convincing interpretation has the γ-carboxylate group making no hydrogen-bond interaction with the protein whilst the α-carboxylate group hydrogen bonds via a water molecule to the side-chain of Gln-35; no interaction of the α-carboxylate with Arg-70 (cf. Arg-57ec) is observed. This is somewhat surprising, given that α-substitution of MTX increases the K_i by about 10^5 [18], consistent with an ionic interaction of the α-carboxylate with, for example, Arg-70. As the MTX complex was prepared by the soaking of pre-grown DHFR/NADPH/TMP crystals in the inhibitor, it is possible that packing constraints within the crystal are preventing either rearrangement of protein side-chains (improbably, given the presence of a large solvent-filled cavity in this region) or a more substantial conformational change.

3.3. *Human dihydrofolate reductase*

The high sequence homology of 89% between mouse L1210 DHFR [19] and human DHFR [20,21] strongly suggests a close similarity between the two structures; this is confirmed by the modelling of the twenty-one sequence differences of human enzyme into the L1210 structure. Fig.3 indicates the locations of the side-chains substituted in human enzyme.

The model shows that of the twenty-one amino acid differences (table 2) from mouse L1210 DHFR, nineteen occur in solvent-accessible regions on or near the surface of the molecule. Fourteen involve the exchange of one polar residue for another, three replace non-polar residues in mouse DHFR by polar residues in human DHFR, and two replace polar residues in mouse DHFR by glycine in human DHFR. Fourteen of the differences are in loop regions between elements of secondary structure. There are none at the substrate binding site and only one at the NADPH binding site. As can be seen from table 2, many of the side-chains in L1210 DHFR that are different in human DHFR do not interact with other atoms of the protein but project into the solvent region. The human DHFR side-chain substitutions have similarly been modelled to have an extended conformation. In some cases ordered solvent exists around DHFR which has to be modified in the human enzyme, owing to differing side-chain length or hydrogen-bonding capability. An example is Glu-127 which changes to His-127 in human

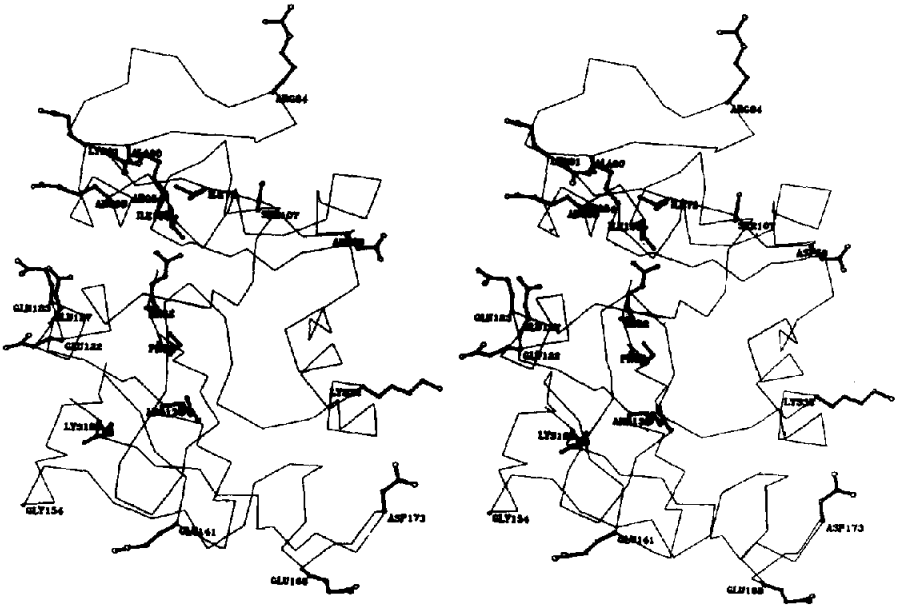

Fig.3. Stereo-view of mouse DHFR molecule, showing the 21 side chains that are replaced in human DHFR.

Table 2
Human DHFR: sequence changes from mouse L1210 DHFR

Location	Mouse	Human	Position[a]	Main side-chain contacts in	
				Mouse	Human
2	Arg	Gly	s	solvent	–
3	Pro	Ser	s	solvent	Lys-132 or solvent
32	Lys	Arg	s	solvent	solvent
54	Arg	Lys	s	2′-phosphate of NADPH	2′-phosphate of NADPH
69	Asp	Gly	s	solvent	–
73	Ile	Leu	i	Ile-100	Thr-100
84	Arg	Gln	s	solvent	solvent
90	Ala	Ser	p	4A from main-chain 95/96	H.bond to >C=O of 92
91	Lys	Arg	s	solvent	solvent
98	Arg	Lys	s	solvent	solvent
100	Ile	Thr	i	Ile-73	Leu-73 & H.bond to >C=O of 96
107	Ser	Asn	p	solvent	Nδ H.bond to >C=O of 104 & of 105
122	Glu	Lys	s	solvent	solvent
123	Gln	Glu	s	solvent	solvent
127	Glu	His	s	solvent	solvent; displaces one water
132	Arg	Lys	s	solvent	solvent, or OH of Ser-3
141	Glu	Asp	s	solvent	solvent
154	Gly	Glu	s	–	solvent
168	Glu	Asp	s	solvent	solvent
173	Asp	Lys	s	solvent	solvent
185	Lys	Asn	s	solvent	solvent

[a] s, surface residue; p, partly buried residue; i, internal residue

DHFR, the Nε2 atom of which displaces one of the L1210 water molecules and could hydrogen bond via another water to Glu-123.

Two differences, 90 and 107, are at partly buried sites. Ala-90 is replaced by Ser-90 whose hydroxyl group can donate a hydrogen bond to the backbone carbonyl group of residue 92. Whilst Ser-107 makes no hydrogen bond in mouse L1210 DHFR, Asn-107 in human DHFR can make hydrogen bonds between its Nδ and the backbone carbonyls of 104 and 105 and between its Oδ and a nearby water.

Ile-73 to Leu and Ile-100 to Thr are the only two sequence differences in regions inaccessible to solvent. They lie adjacent to each other in mouse DHFR in a hydrophobic environment. Replacement of Ile-100 by the smaller Thr-100 in human DHFR gives rise to a decrease in packing density and a number of orientations for Leu-73 and Thr-100 are then possible. The effect of the polar residue in this hydrophobic environment can be reduced by allowing the hydroxyl group of Thr-100 to donate a hydrogen bond to the backbone carbonyl of residue 96.

The single difference at a ligand binding site is the conservative substitution of Lys-54 in human DHFR for Arg-54. The ε-amino group of Lys-54 can interact with the 2′-phosphate of NADPH in place of the guanidinium group of Arg-54.

4. CONCLUSIONS

The refined structures reported above give

details of how certain antifolate drugs interact with a mammalian DHFR. The observed differences in TMP and enzyme conformation between mouse L1210 DHFR and chicken DHFR relate primarily to the substitution of Phe-31 for Tyr-31. Comparison with *E. coli* DHFR reveals that TMP bound to L1210 DHFR is in a significantly different conformation, and that fewer interactions between the diaminopyrimidine moiety and the protein are present, consistent with the drug's lower affinity for L1210 enzyme. In contrast, with MTX, equivalent interactions occur between the pteridine group and either enzyme. The distinct Phe-31 conformation in the mouse DHFR/MTX ternary complex requires an orientation of the *p*-aminobenzoyl glutamate moiety altered from that observed in bacterial DHFR/MTX complexes. Further studies are required to assess the significance of this observation.

The human DHFR model, derived by fitting the human amino acid sequence to the mouse L1210 DHFR structure, shows no steric hindrances, and the changes in electrostatic interactions are minor and remote from the substrate binding site. Although possible small changes in vibrational modes which might affect catalytic activity cannot be discounted, we conclude that the structure of the mouse L1210 enzyme around the substrate binding site represents a good model of human DHFR for use in drug design.

ACKNOWLEDGEMENTS

We are grateful to Mr A. Angell, Mrs R.C. Castle, Mr C.K. Ross and the late Mrs N. Padia for their assistance, and to Drs P.J. Goodford, L. Kuyper, and B. Roth for helpful discussion. We thank the Medical Research Council for support (grant G8311250 to A.J.G. and A.C.T.N.).

REFERENCES

[1] Blakley, R.L. (1969) The Biochemistry of Folic Acid and Related Pteridines (Frontiers in Biology, 13), North Holland, Amsterdam.
[2] Baccanari, D.P., Daluge, S. and King, R.W. (1982) Biochemistry 21, 5068–5075.
[3] Hitchings, G.H. and Smith, S.L. (1980) Adv. Enzyme Regul. 18, 349–371.
[4] Baker, D.J., Beddell, C.R., Champness, J.N., Goodford, P.J., Norrington, F.E.A., Smith, D.R. and Stammers, D.K. (1981) FEBS Lett. 126, 49–52.
[5] Bolin, J.T., Filman, D.J., Matthews, D.A., Hamlin, R.C. and Kraut, J. (1982) J. Biol. Chem. 257, 13650–13662.
[6] Volz, K.W., Matthews, D.A., Alden, R.A., Freer, S.T., Hansch, C., Kaufman, B.T. and Kraut, J. (1982) J. Biol. Chem. 257, 2528–2536.
[7] Matthews, D.A., Bolin, J.T., Burridge, J.M., Filman, D.J., Volz, K.W., Kaufman, B.T., Beddell, C.R., Champness, J.N., Stammers, D.K. and Kraut, J. (1985) J. Biol. Chem. 260, 381–391.
[8] Champness, J.N., Stammers, D.K. and Beddell, C.R. (1986) FEBS Lett. 199, 61–67.
[9] Matthews, D.A., Smith, S.L., Baccanari, D.P. and Burchall, J.J. (1986) Biochemistry 25, 4194–4204.
[10] Roberts, G.C.K. (1983) Chemistry and Biology of Pteridines (Blair, J.A. ed.) pp.197–214, Walter de Gruyter, Berlin.
[11] Birdsall, B., Roberts, G.C.K., Feeney, J., Dann, J.G. and Burgen, A.S.V. (1983) Biochemistry 22, 5597–5604.
[12] Champness, J.N., Kuyper, L. and Beddell, C.R. (1986) Topics in Molecular Pharmacology (Burgen, A.S.V. et al. eds) vol.3, pp.335–362, Elsevier, Amsterdam.
[13] Stammers, D.K., Champness, J.N., Dann, J.G. and Beddell, C.R. (1983) Chemistry and Biology of Pteridines (Blair, J.A. ed.) pp.567–571, Walter de Gruyter, Berlin.
[14] Arndt, U.W., Champness, J.N., Phizackerley, R.P. and Wonacott, A.J. (1973) J. Appl. Crystallogr. 6, 457–463.
[15] Hendrickson, W.A. and Konnert, J.H. (1980) Biomolecular Structure, Function, Conformation and Evolution (Srinivaran, R. ed.) vol.1, pp.43–57, Pergamon Press, Oxford.
[16] Jones, T.A. (1978) J. Appl. Crystallogr. 11, 268–272; (1982) in: Computational Crystallography (Sayre, D. ed.) pp.303–317, Clarendon Press, Oxford.
[17] Matthews, D.A., Bolin, J.T., Burridge, J.M., Filman, D.J., Volz, K.W. and Kraut, J. (1985) J. Biol. Chem. 260, 392–399.
[18] Piper, J.R., Montgomery, J.A., Sirotnak, F.M. and Chello, P.L. (1982) J. Med. Chem. 25, 182–187.
[19] Stone, D., Paterson, S.J., Raper, J.H. and Phillips, A.W. (1979) J. Biol. Chem. 254, 480–488.
[20] Masters, J.N. and Attardi, G. (1983) Gene 21, 59–63.
[21] Pan, Y.-C.E., Domin, B.A., Li, S.S.-L. and Cheng, Y.-C. (1983) Eur. J. Biochem. 132, 351–359.